Metrol. Meas. Syst., Vol. 33 (2026) No. 1, pp. 1–17
DOI: 10.24425/mms.2026.158370

PAN POLSKA AKADEMIA NAUK

METROLOGY AND MEASUREMENT SYSTEMS
Index 330930, ISSN 0860-8229
www.metrology.wat.edu.pl

M&MS

INTERFERENCE DUE TO THERMAL RADIATION IN LOSS MEASUREMENTS DURING FIRE TESTS OF OPTICAL FIBER CABLES

Krzysztof Borzycki

National Institute of Telecommunications, ul. Szachowa 1, 04-894 Warsaw (✉ *k.borzycki@il-pib.pl*)

Abstract

Certain applications of fused silica optical fibers, in particular fire-resistant cables and sensors working in hot environments (*e.g.*, nuclear reactors) require short- or long-term operation at temperatures exceeding 800 °C. Peak temperatures during fire tests of fire-resistant cables vary between 830 °C and 1040 °C depending on applicable standards. If the fiber contains OH^- ions and hydrogen, it exhibits both increased loss and incandescence in the corresponding absorption bands. Additionally, deteriorated fiber with multiple cracks and other microscopic defects collects radiation from glowing surroundings. During loss measurements with a standard setup including a light source and a power meter, thermal radiation from both sources adds to radiation from the light source, causing false decrease of indicated fiber loss. Several methods to eliminate this interference are presented.

Keywords: fused silica optical fiber, fire-resistant cable, loss measurement, fire test, incandescence.

1. Introduction

Fire-resistant fiber optic cables provide connectivity for safety systems, video monitoring, and emergency communications and are required to retain optical continuity during fire for 15–120 minutes [1–3]. Such cables incorporate standard telecom fibers made of fused silica. Resistance to fire is tested in simulated fire conditions using gas burners. *International Electrotechnical Commission* (IEC) tests involve temperatures around 840 °C [1], while maximum temperature stipulated in the German DIN 4102-12 [2] standard exceeds 1000 °C after 90 minutes, in accordance with data for "cellulosic" fire given in the ISO 834-1 standard [3]. The loss of fibers is monitored [4], and its permitted rise during the fire test is limited to [5]:

– 1 dB/m at 1550 ± 10 nm for single mode fibers [6],
– 2 dB/m at 1300 ± 20 nm for multimode mode fibers [7].

Fused silica fibers heated to temperatures above 800 °C both glow (incandesce) and collect thermal radiation emitted by the surrounding matter – usually soot left from thermal decomposition of polymeric tubes and fiber coatings. Incandescence consists of several spectral peaks associated

Article history: received October 24, 2025; revised January 9, 2026; accepted January 30, 2026; available online March 13, 2026.

with OH^- (hydroxyl) ions present in fused silica. It fades over time during heating, as the hydroxyl ions break down:

$$2(\equiv \text{Si–OH}) \leftrightarrow (\equiv \text{Si–O–Si} \equiv) + H_2O, \tag{1}$$

$$2(\equiv \text{Si–OH}) \leftrightarrow 2(\equiv \text{Si–O} \equiv) + H_2 \tag{2}$$

and the resultant hydrogen and water vapor diffuse out of the fiber [8, 9]; this process is sometimes referred to as "fiber drying". Collected radiation is broadband, with spectral distribution close to a perfect blackbody radiator, and its intensity increases over time due to the growing number of microscopic cracks and cristobalite (crystalline form of SiO_2) inclusions serving as optical couplers [9] and crack initiators.

Thermal radiation distorts results of loss measurements performed with a *Light Source and Power Meter* (LSPM) setup. It adds to the test signal from a light source; the power meter indicates higher power and lower fiber loss than without it. This can lead to acceptance of fire test result being in fact negative, with excessive fiber loss or even a fiber break.

This situation is an exception in optical fiber cable testing, where the absence of interference from internally generated or collected radiation is normally assumed. The only other case of meaningful interference is in multi-wavelength loss measurements, where wavelength division multiplexers with a high level of crosstalk ($-30 \ldots -20$ dB) are often used.

In the following sections, we present sources, spectra and powers of thermal radiation emerging from hot optical fibers (Section 2), resulting errors in measurements of fiber loss under such conditions (Section 3), and some methods of eliminating them (Section 4), recommended by the author after gaining experience with monitoring of fiber loss in a cable during a fire test. Conclusions are presented in Section 5.

2. Thermal radiation in fibers under fire conditions

2.1. Fibers under tests and test procedures

All optical characteristics presented in this paper, except for Section 2.2, have been measured during high temperature experiments at the National Institute of Telecommunications on telecom fibers belonging to three classes:

1. modern single mode fibers with low content of hydroxyl ions, conforming to the current ITU-T standards G.652.D and G.657.A2 (2 types of fibers),
2. old (1990–1993) single mode fibers with high content of hydroxyl ions, conforming to the old ITU-T standard G.652.A (3 types of fibers),
3. modern 50/125 µm multimode fibers of OM2 and OM3 types (3 types of fibers).

During most tests, a single fiber was placed directly in an electric oven having a 1 m long hot zone with a ceramic tube and protected by a fused silica tube. This tube was not sealed, so during the test, polymeric fiber coatings first carbonized at 350–450 °C and later burned out at 500–600 °C. To investigate the effects of carbon char surrounding optical fibers during the fire test, the fiber was placed in a stainless steel tube having a 1 mm inner diameter with sealed ends and the carbon char produced by pyrolysis of the coating did not burn.

For optical measurements, a 3–4 m long fiber sample was fusion spliced to a pigtail with an FC/PC connector at one end (for measurements of radiation power and spectra). The other end was protected against the entry of light. Variations in loss at high temperatures were tested separately on selected samples spliced to pigtails at both ends, using laser sources (850, 1310 and 1550 nm) and an optical power meter, as described in Section 3.1.

Fibers under test were normally subjected to temperatures rising from room temperature up to 1000 °C. Beginning from 400 °C, the temperature was raised in fixed 50 °C steps. Measurements of power of thermal radiation from single-mode fibers were possible starting from 400–450 °C and required darkroom conditions. Optical spectra of radiation from fibers (2) and (3) were normally measured at 800, 900 and 1000 °C. Radiation emitted from fibers belonging to class (1) was too weak for spectral measurements.

Experiments with several samples were repeated 2 or 3 times to observe fiber "drying" and deterioration, and/or to measure fiber loss. Progressive drying and deterioration of the fiber caused differences between the results of repeated tests mentioned in Sections 1 and 2.3–2.6. Additional time required for spectral measurements resulted in detectable skips on the recorded power vs. temperature graph. Those phenomena are of limited importance for fire tests, which are short and cable samples are tested only once. The situation is different during operation of fiber sensors, not covered here.

Detailed characteristics of radiation emerging from fused silica fibers held at temperatures up to 1000 °C: power, spectral distribution, variation over time, and physical mechanisms responsible are presented in the paper [10]. This chapter includes a summary and examples needed to understand the characteristics of optical interference encountered during fire tests of optical fiber cables and in high temperature fiber sensors.

2.2. Absorption bands of hydroxyl ions in fused silica ("water peaks")

Table 1 shows central wavelengths, relative intensity of absorption, and spectral width at half-maximum (FWHM) for water peaks in the 700–1700 nm range of interest for fiber optic measurements, based on data from [11]. The wavelengths corresponding to four components of the 1390 nm absorption peak increase reversibly by 7 nm when temperature increases from 20 °C to 800 °C [12]. Hydroxyl absorption is little affected by the details of preform making and fiber drawing operations, and the spectral data are quite accurate. However, the optical attenuation coefficients per ppm of OH^- in the glass reported in the literature differ considerably [11].

Table 1. Strongest hydroxyl absorption bands of fused silica between 700 and 1700 nm.

Central Wavelength [nm]	**Relative Intensity [dB]**	**σ Parameter [nm]**	**FWHM (2.355 σ) [nm]**
724	–29.1	—	—
825	–42.2	—	—
878	–28.9	—	—
943	–16.1	—	—
1139	–29.5	—	—
1246	–13.7	≈ 10.7	≈ 25.3
1353	–10.6	20.2	47.5
1382	0.0	6.7	15.8
1393	–2.4	10.6	25.0
1407	–7.0	29.2	68.8

The intensity of the strongest, combined peak at 1390 nm (actually four combined peaks at 1353/1382/1393/1407 nm, see Fig. 1) rises with temperature in accordance with the Arrhenius formula, with a reported activation energy of 1.13 eV [13] or 0.82 eV [9]. Attenuation at 1390 nm

increases at the same rate and reaches 5–8 dB/m at temperatures in the range of 900–1000 °C [8,10] – see Fig. 6. In such conditions, the power of the accumulated incandescent radiation is self-limiting, or "saturating" in a fiber longer than approximately 0.5 m; this length is shortened with increasing temperature. Fiber attenuation at wavelengths away from "water peaks", *e.g.*, 1300 nm is little affected.

The strongest absorption (and incandescence) bands are shown in Fig. 1. The measured spectra of the fiber's incandescence (Figs. 2 and 3) show only the combined peak at approximately 1390 nm and a much weaker one at 1246 nm. Interestingly, the next strongest peak at 943 nm, well known as the loss peak in multimode fibers, was almost undetectable during our measurements due to internal noise of the optical spectrum analyzer.

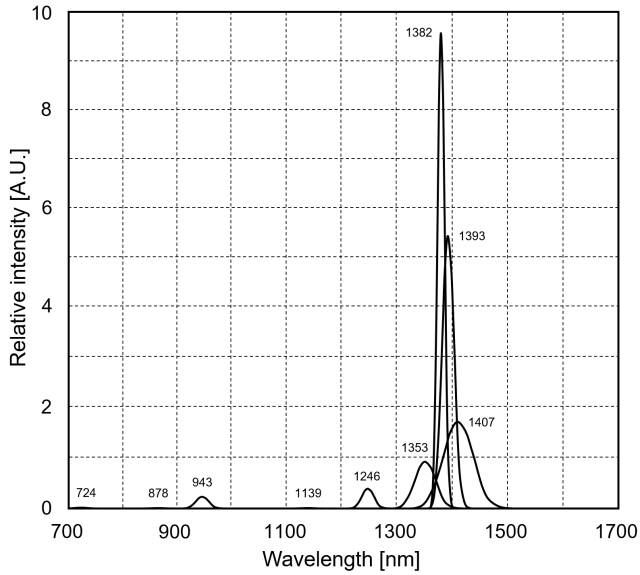

Fig. 1. Main absorption bands of fused silica contaminated with hydroxyl ions. This graph is based on data from the paper [11]. The spectral range corresponds to the measured spectra presented in Figs 2, 3, 5 and 6.

2.3. Incandescence of hot optical fiber

Figures 2 and 3 show the spectra of radiation emitted by:
– a 50/125 µm graded index multimode fiber, and
– a single mode fiber conforming to the old ITU-T G.652.A Recommendation [14],
respectively, measured in our laboratory. The samples were 1 m long and heated to 900 °C shortly before the measurements. The fibers were tested in air inside a ceramic tube. Their coatings had been fully burned out before, and the power of coupled radiation (Sections 2.4 and 2.5) was low, but still detectable.

The spectra were measured with a Yokogawa AQ-6315B optical spectrum analyzer. Due to low power exiting test fibers and relatively large spectral widths of "water peaks" (Table 1), resolutions of 5 nm or 10 nm were selected. This, together with large spectral widths of four strongest emission peaks at 1353 nm, 1382 nm, 1393 nm and 1407 nm [8], made them appear as a single peak of irregular shape – see Fig. 2. The total power of radiation exiting fiber under test was measured with an HP 8152A optical multimeter and an HP 81532A InGaAs power sensor sensitive in the 800–1700 nm spectral range.

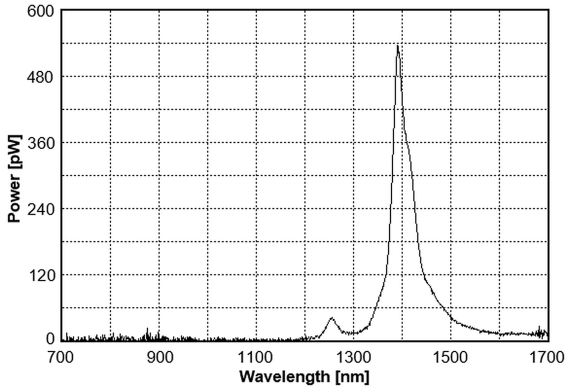

Fig. 2. Spectrum of thermal emission of OM2 multimode fiber at 900 °C, total power: –49.39 dBm.

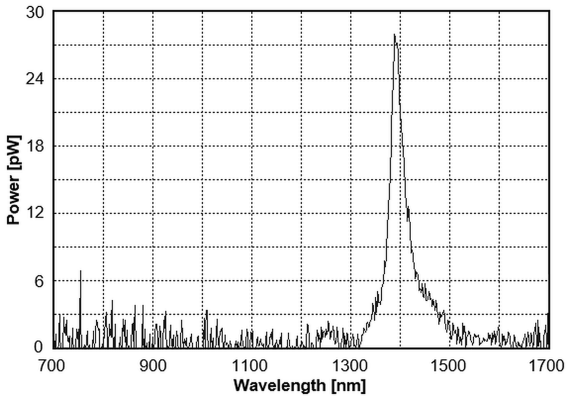

Fig. 3. Spectrum of thermal emission of G.652. A single-mode fiber at 900 °C, total power: –66.71 dBm.

The incandescence of a single mode fiber, even one exhibiting water peaks (ITU-T G.652.A) is substantially weaker than that of the 50/125 µm OM2/OM3/OM4 multimode fiber; actual values measured in our experiments varied considerably. The factors influencing the intensity of thermal radiation that exits hot fiber are listed and explained in Section 2.6.

Incandescence spectra were very similar for single-mode and multi-mode fibers, except for power levels, and in agreement with data in Table 1.

2.4. Thermal radiation coupled into the fiber

The strongest mechanism of coupling of external radiation into the fiber involves reflections of this radiation by cracks penetrating the fiber's cladding and core at varying angles, created when microscopic inclusions of cristobalite (crystalline, a denser form of silica) appear on the surface of the fiber [15–17]. Because specific gravity of cristobalite (2.35) is higher than that of fused silica (2.20), local loss of about 6% material volume produces extreme strain and initiates glass breaks. A microscope photograph of fiber damage is shown in Fig. 4. Two cracks of uneven width and directions extend from this location. Identified pieces of dust were retouched to improve image clarity. More data can be found in [10].

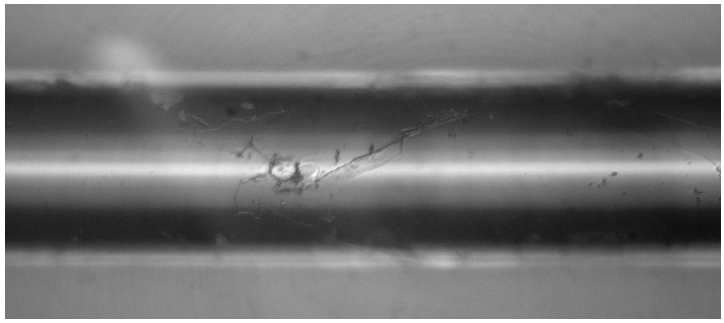

Fig. 4. Surface defect in an optical fiber (circular feature) after 4.5 h of heating to 900–1000 °C, area shown: 200 × 500 µm.

Due to different refractive indices of fused silica (1.46) and air (1.00), a crack reflects about 4% of impinging radiation at an angle dependent on crack direction. A part of external radiation is directed at the fiber acceptance angle, while part of radiation propagating in the fiber is lost. Other defects in fiber core or at the core/cladding interface, such as inclusions, gas bubbles, or defects produced by γ-radiation [18] also facilitate coupling of external radiation. A weak coupling, increasing with duration of heating, was observed also in fibers exhibiting no visible cracks – see [10], in particular Figs. 8 and 15 there.

Infrared radiation collected by deteriorated fiber is considerably stronger than that produced inside fiber by incandescence, even with a high content of hydroxyl ions.

2.5. Evolution of radiation spectrum over time

When optical fiber is subjected to high temperature (≥ 800 °C) for a duration typical of fire, defined in EN 50575 [19] as 15–120 minutes, two concurrent changes occur over time:

– a decrease in (narrowband) fiber incandescence due to fiber "drying" (Chapter 1),

– an increase in (broadband) radiation coupled into the fiber with its deterioration (Section 2.4).

Initially, the spectrum is composed of several peaks (Fig. 1, 2, and 3), but a continuous, long-wavelength component steadily rises and eventually dominates in strongly deteriorated fiber (Fig. 5). Changing spectrum and power make it impossible to establish power vs. temperature characteristics for a given fiber, thus the results of repeated tests differ [10].

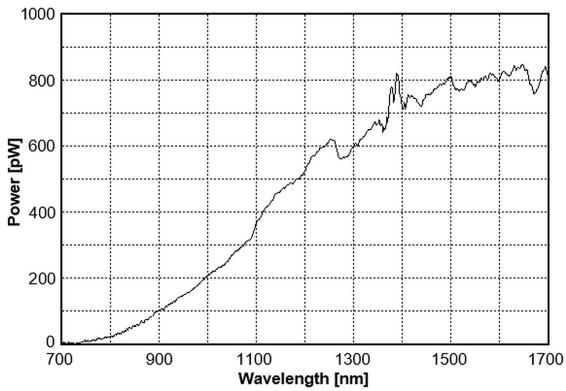

Fig. 5. Spectrum of coupled thermal emission of an OM2 multimode fiber at 1000 °C. The fiber exhibited localized escape of light due to cracks but retained optical continuity. Total power: –39.79 dBm.

Metrol. Meas. Syst., Vol. 33 (2026), No. 1, pp. 1–17
DOI: 10.24425/mms.2026.158370

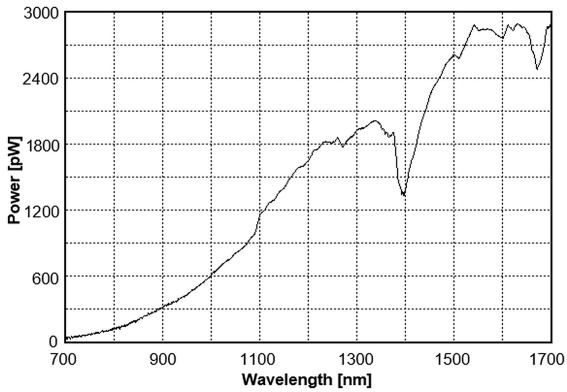

Fig. 6. Spectrum of thermal emission of carbon soot collected by the cleaved end of an OM2 multimode fiber at 1000 °C. The fiber placed in the hot zone was 0.3 m long and exhibited an attenuation of approximately 2 dB at 1390 nm. Total power: -33.38 dBm.

2.6. Power of thermal radiation exiting hot fiber

Table 2 shows power ranges of incandescent and coupled radiation emerging from a 1 m long fiber sample held at 900 °C, measured in the 800–1700 nm spectral range for each fiber class defined in Section 2.1. Incandescent radiation was measured in fibers heated in air, with all coatings burned out. The absence of coupled radiation was confirmed by spectral measurements. All measurements were performed approximately 5 minutes after the temperature of 900 °C was reached, before a significant change in incandescence over time (Section 2.3) took place. Coupled radiation was measured in fibers surrounded by carbon soot and protected against the access of oxygen by a stainless steel tube. The results for different fibers from each class varied up to 7 dB for the reasons listed below.

Table 2. Typical powers of incandescent and coupled radiation at 900 °C.

Fiber Type and Standard	**Incandescent Radiation [dBm]**	**Coupled Radiation [dBm]**
Single mode without a water peak [G.652.D, G.657.A2]	−85 . . . − 81	–60
Single mode with a water peak [G.652.A]	−71 . . . − 66	–56
50/125 µm multimode (OM2 and OM3)	−57 . . . − 50	–42

In general, the intensity of thermal radiation that exits the fiber depends primarily on five factors:

1. Core cross-section because total power of incandescent radiation is proportional to the volume of hot glass. Comparing single-mode and multimode fibers, the power of radiation generated in a multimode fiber with 50 µm core is about 30 times (15 dB) higher than in a single-mode fiber having ≈ 8.3 µm core diameter and ≈ 9.5 µm *mode field diameter* (MFD) [6, 7, 14]. Multimode fiber has also higher GeO_2 (germania) content in the core – this doping increases emissivity of fused silica. For the same OH^- content and temperature, at least 72-fold (18.6 dB) higher incandescent power can be expected in multimode fiber. Additionally, 50/125 µm multimode fiber has a higher numerical aperture: 0.14 vs. 0.20, and the proportion of omnidirectionally emitted thermal radiation accepted by multimode fiber is twice as large.

2. Glass emissivity is proportional to its absorption. Of primary importance is the component of fiber attenuation associated with the hydroxyl (OH^-) content in the glass of which the fiber core is made. The difference between the intensity of incandescence in a typical pre-1999 single mode fiber (ITU-T G.652.A) with an added loss of ≈ 1 dB/km at the water peak wavelength (≈ 1390 nm, Table 1) and the current low-OH fiber (ITU-T G.652.D) with the same loss below 0.05 dB/km is by a factor of 20–100 (13–20 dB). Multimode fibers have a higher OH^- content than single mode ones and their incandescence observed in our experiments was about 20 times (13 dB) stronger than in the old G.652. A single mode fiber [10], as seen in Figures 2 and 3.

3. Fiber temperature – the intensity of incandescence of fiber increases with temperature [9,13], while the spectrum does not change (Section 2.2). The intensity of radiation from carbon soot also rises, but with a shift of the peak to shorter wavelengths. An example is shown in Fig. 7.

4. Thermal history of the fiber: heating causes gradual destruction of hydroxyl ions and out-diffusion of resulting hydrogen through the cladding (Chapter 1). Incandescence fades over time due to the ongoing destruction of OH^- ions and the escape of resultant H_2 and H_2O through the cladding [8]. A 50% (3 dB) reduction of radiation intensity was observed after 1–2 hours at 1000 °C; it was slower in fiber with a fluorine-doped layer around the core [10].

5. Density of surface defects and cracks in the fiber (Section 2.4), which increases with duration and temperature of heating. More cracks and defects mean a more efficient coupling of external radiation into the fiber's core when some defects reflect radiation into the acceptance cone of the fiber core. While at the beginning of a high temperature test the broadband (blackbody-like) radiation observed at the end of the fiber is almost absent (Fig. 2), it gradually gets more intense and dominates in strongly degraded fiber (Fig. 5).

6. Carbonization of the fiber coating and tube and later burning of this carbon (only in air). The result is a marked increase in coupled radiation at temperatures starting from 450 °C, permanent in an oxygen-free environment [10].

Measured spectra and powers of thermal radiation are relatively consistent for fibers belonging to a given class defined in Section 2.1, and when the test conditions: temperature, heating duration, surrounding material, access of air are identical. The exception was rapid, often in less than 1 minute, deterioration of some multimode fibers at temperatures between 900 and 1000 °C, resulting in the total loss of optical continuity and strong coupled radiation: −36 . . . − 33 dBm with the broadband spectrum.

For a 3 m long cable and fiber in the fire zone, which is the minimum length required in DIN 4102-12, the values listed in Table 2 still apply because of the self-limiting effect (Section 2.2). The power of thermal radiation emerging from a 3 m long 50/125 µm multimode fiber heated to 1000 °C measured during the actual fire test of the cable was approximately –36 dBm.

Figure 7 shows the power of thermal radiation emerging from a 1 m long straight sample of 50/125 µm OM2 multimode fiber surrounded by carbon char (soot) left from pyrolysis of the fiber coating and the 0.9 mm thick buffer in the absence of oxygen as a function of temperature, measured in the laboratory. This can be assumed to be the maximum level of interference expected during fire tests on fire-resistant cables. The fiber under test was placed in a thin stainless steel tube sealed at both ends to simulate conditions inside a fire-resistant cable where the polymer tube with fibers is surrounded by mica tapes blocking access of air and burn-out of carbon.

Metrol. Meas. Syst., Vol. 33 (2026), No. 1, pp. 1–17
DOI: 10.24425/mms.2026.158370

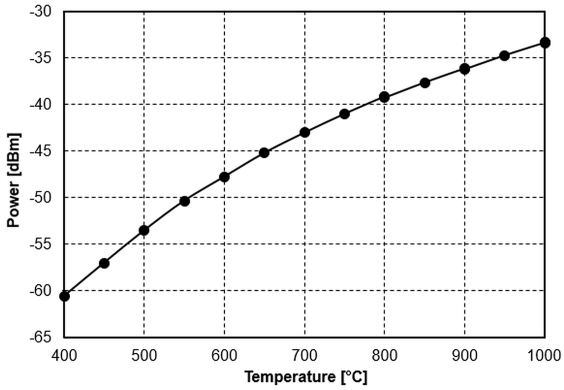

Fig. 7. Power of thermal radiation from an OM2 multimode fiber surrounded by carbon soot vs. temperature.

3. Interference during measurements of fiber loss

3.1. LSPM method for fiber loss testing

Variations in fiber loss (attenuation) during the fire testing of the cable are normally measured using a *Light Source and Power Meter* (LSPM) setup shown in Fig. 8. More elaborate setups can include fiber switches for monitoring multiple fibers or multiple light sources and *Wavelength Division Multiplexing* (WDM) multiplexers for simultaneous measurements at several wavelengths.

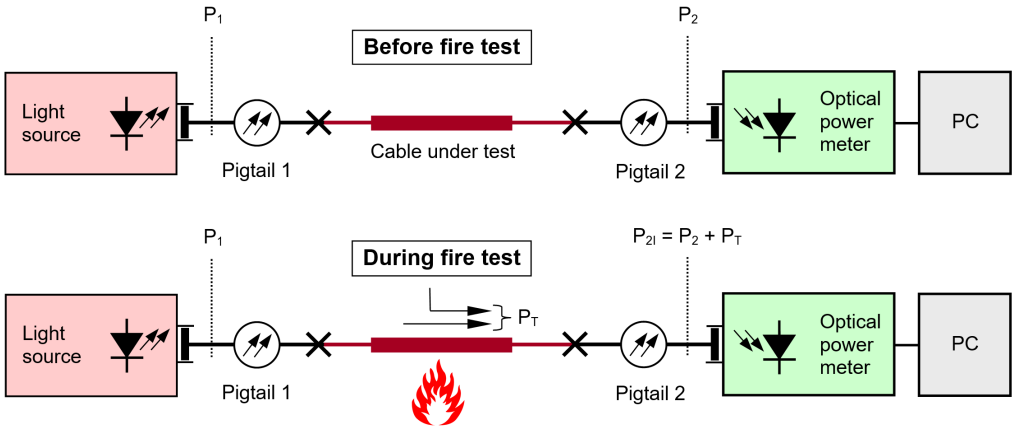

Fig. 8. LSPM setup for measuring and recording variations in attenuation (loss) of optical fiber in a cable during a fire test. The fiber under test is fusion spliced into pigtails for connections to the test instruments.

This method is designated “Method B” in the EN-60793-1-40 standard for measurements of absolute fiber loss [20]. The monitoring of loss changes with a similar setup is covered by EN60793-1-46 [21] and named "Method A". It is widely accepted for cable tests. However, during a fire test, thermal radiation adds to the radiation launched into the fiber under test from the light source. The indicated power is higher, and the loss lower than the true one.

3.2. Interference during measurements with the LSPM setup

The optical path between the light source and the optical power meter (Fig. 8) includes a relatively short fiber under test encased in the cable subjected to fire; its *initial loss* (IL_F) can change during the test. The combined loss of all other passive components of the optical path: lengths of fibers outside the fire zone, splices, connectors, switches, splitters, or filters (IL_C) is substantially higher than IL_F – up to 20 dB in some cases.

First, it is assumed that IL_C has a fixed value during the test, and variations in the measured power are caused only by changes in IL_F. Second, it is assumed that all radiation present in the fiber under test originates from the light source, which launches radiation characterized by a stable power (P_1) and wavelength, so variations of optical power exiting the fiber (P_2) and measured with an optical power meter can be directly converted to the change in fiber attenuation (IL_F).

Using the logarithmic scale of power (dBm) and loss (dB), we have the following formulae for the power reaching the input port of the optical power meter (P_2):

$$P_2 = P_1 - (IL_F + IL_C) \tag{3}$$

and measured variations in fiber loss (ΔIL_C):

$$\Delta IL_C = -\Delta P_2, \tag{4}$$

where ΔIL_C and ΔP_2 are variations of the respective parameters from the initial values.

As presented in Section 2, hot fibers generate and collect radiation, which adds to radiation launched from the light source, as shown in Fig. 8. If no special modifications are made to the LSPM setup, the optical power meter shows a sum of:

- the true test power (P_2), launched from the source and attenuated on the way to the power meter,
- power of interfering thermal radiation (P_T), indicating a value of P_2 distorted by optical interference (P_{2I}):

$$P_{2I} = P_2 + P_T \tag{5}$$

(for power values in W), or

$$P_{2I} = 10\log\left[10^{\left(\frac{P_2}{10}\right)} + 10^{\left(\frac{P_T}{10}\right)}\right] \tag{6}$$

(for power values in dBm).

As a result, the indicated power increases and the indicated fiber loss decreases. The *error in loss indication* (ErrIL) (value in the logarithmic scale, dB) depends on the ratio of powers P_T and P_2 (values in the linear scale):

$$\mathrm{Err}IL = 10\log[(P_2 + P_T)/P_2] = 10\log[(P_T/P_2) + 1] \tag{7}$$

or, when the logarithmic scale is used exclusively:

$$\mathrm{Err}IL = 10\log\left[10^{\left(\frac{P_T - P_2}{10}\right)} + 1\right]. \tag{8}$$

Examples of errors in power/loss measurements are shown in Table 3. For example, for a 0.01 dB permitted error, –36 dBm thermal radiation power in 50/125 µm multimode fiber, and a 16 dB loss rise to be measured during the test (2x the limit for a 4 m fiber in a fire zone), the power launched into the fiber under test must exceed +6.4 dBm. This "brute force" solution is effective but requires an expensive high-power light source for multimode cables.

Table 3. Error in fiber loss indication (Err*IL*) as a function of the test signal (P_2) to the interference ratio (P_T).

Err*IL* [dB]	P_T/P_2	P_2/P_T	P_2/P_T [dB]
1.00	0.2589	3.86	5.87
0.50	0.1220	8.20	9.14
0.20	0.0471	21.23	13.27
0.10	0.0233	42.92	16.33
0.05	0.0116	86.21	19.36
0.02	0.0046	216.65	23.36
0.01	0.0023	433.79	26.37

During a fire test performed according to DIN 4102-12 [2], the author observed that intense thermal radiation at temperatures around 1000 °C completely masked the increase of fiber loss, and even the total loss of fiber continuity in the cable under test, producing an erroneous impression of stable or even decreasing loss. Examples of such power and loss measurements for one fiber in a cable under test are shown in Figs. 9 and 10. In order to measure 8 fibers, the light from a single source was divided by means of an optical 1:8 splitter, which reduced the launched power by approximately 10 dB with respect to direct connection.

During this test, the loss measurements started 20 minutes before the ignition of the burners in the fire chamber. The gaps between the measurement data result from sequential switching of the power meter input to 8 fibers in the cables under test; the full switching cycle was 160 s long.

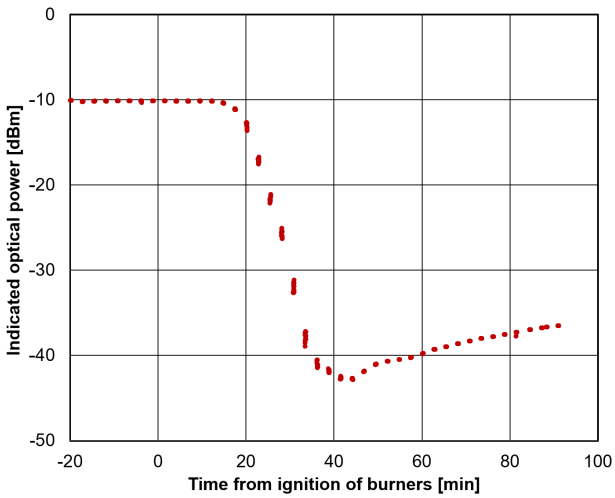

Fig. 9. Indications of optical power during the cable fire test of a cable according to DIN 4102-12. Measurements of single multimode OM2 fiber with 33 m length passing through the fire zone.

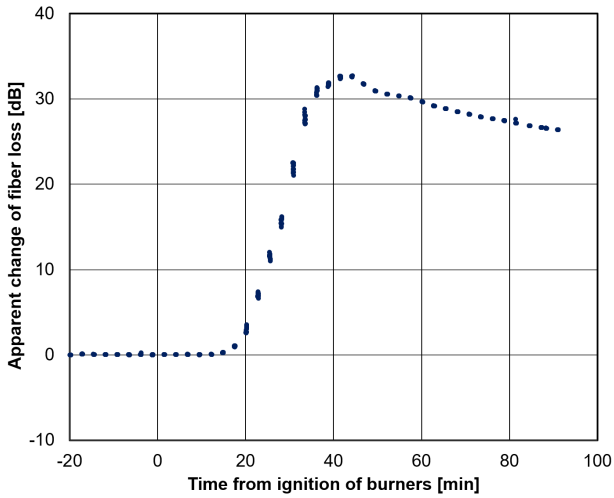

Fig. 10. Evolution of fiber loss over time calculated from the power measurements shown in Fig. 9.

At the end of this test, the power indicated by the optical power meter with 0.01 dB resolution did not change after the deactivation of the light source, because thermal radiation (P_T) was much stronger than the attenuated test signal (P_2), as shown in Fig. 11. Due to a confidentiality agreement, more details of this test cannot be published.

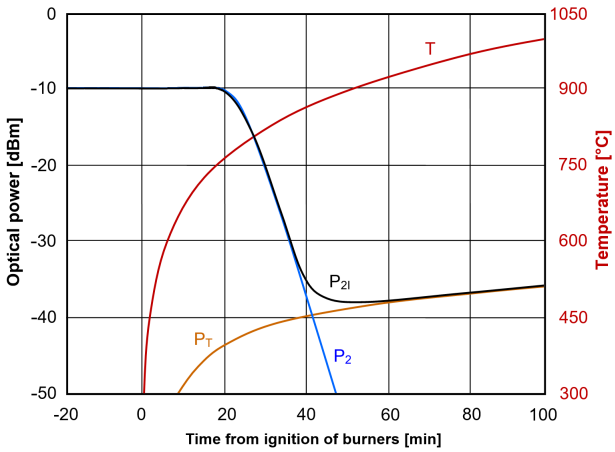

Fig. 11. Evolution of temperature (T), and optical powers P_2, PT, and P_2I over time during a fire test, explaining the results shown in Figs. 9 and 10.

On the other hand, interference from thermal radiation encountered during fire tests performed in accordance with EN 50200 [1] and EN 50282 [4] was negligible due to:

– lower maximum temperature: 840 °C instead of 1040 °C, and 6–8 dB weaker thermal radiation [10]), as shown in Fig. 7,

– 10 dB higher optical power launched into the fiber under test, because no 1:8 splitter was used on the light source side of the test setup.

4. Elimination of interference from thermal radiation in LSPM loss measurements

The following methods can be recommended:

(a) Use of a high power light source to increase the signal-to-interference ratio to the value listed in the right-hand column of Table 3 for a required value of Err*IL*.

(b) Suppression of thermal radiation with bandpass filters: 1300 nm for multimode fibers, and 1550 nm for single mode fibers, placed at the input of the power meter (4.1).

(c) Periodic ON/OFF switching of the light source to measure the power of thermal radiation interference (in the OFF state) and subtract it from the power measured in the ON state (4.2). Alternatively, a light source can be used with modulation of the amplitude at a fixed frequency and an optical receiver that responds only to the AC component of optical power (4.3).

(d) Shortening of the fiber under test placed in the fire zone, *e.g.*, including only one fiber from the cable under test in the test circuit. This reduces the maximum loss increase to be measured and increases the minimum expected value of P_2, while the power of thermal radiation is similar due to its self-limitation in the hot fiber.

(e) Adoption of 850 nm or 940 nm for OM5 fibers as test wavelengths for multimode cables instead of 1300 nm, and the use of a power meter with a silicon photodetector, sensitive only to wavelengths below ≈ 1150 nm, and blind to incandescence at 1353/1382/1393/1407 nm (Figs. 1, 2), instead of an InGaAs detector sensitive to wavelengths up to ≈ 1750 nm.

Thermal radiation constitutes a bigger problem during fire testing of multimode cables because:

– the power of thermal radiation is 15–20 dB higher in multimode fibers (Section 2.6),
– the permitted increase in attenuation of the multimode fiber during the fire test is twice the value for the single-mode fiber (2 dB/m vs. 1 dB/m) [4].

Two or more of methods (a)–(d) can be combined for better rejection of interference [17].

P_T is the power indicated when the light source is disconnected (*e.g.*, with a fiber switch) or deactivated, which is not the true power of thermal radiation generated and collected by the fiber under test [17] but is suitable for correction of the test results (Section 4.2).

Testing multimode fibers at 850 nm wavelength is desirable also because their current applications, including CWDM networks with OM5 fibers, are restricted to center wavelengths ≤ 940 nm [22]. Unfortunately, the current IEC standard for testing fiber cables [23] requires loss testing of multimode cables at 1300 ± 20 nm, unless the longest specified operating wavelength is shorter. This standard, however, includes 850 ± 20 nm as an alternative test wavelength.

4.1. Bandpass filtering

An optical bandpass filter with the central wavelength corresponding to one of the sources is placed at the input of the optical power meter. The effectiveness of this method is limited for several reasons:

– the wavelength tolerances of sources (typ. ±10 nm or ±20 nm) and filters (typ. ±10 nm), plus the spectral width of radiation emitted by Fabry-Perot lasers (typ. 5–10 nm) dictate a selection of bandpass 30–50 nm wide, unless the source and filter are spectrally characterized and matched,
– fiber test wavelengths are set in standards, although alternative arrangements between the cable supplier and the user are often permitted. In particular, most standards for testing multimode cables still stipulate loss measurements at a wavelength of 1300 nm, near the "water peaks" (Table 1), and require a wideband InGaAs detector, while all current applications of OM2/3/4/5 fibers are at wavelengths between 850 and 940 nm (nominal values),

– the low-cost bandpass filter often has a too narrow blocking band to filter out thermal radiation across the whole sensitivity range of InGaAs photodetectors, which extends from less than 800 nm to over 1750 nm. Filter specifications must be read with care.

Experiments in our laboratory [17] involved commercial Thorlabs and Edmund Optics filters that had 30 nm, 25 nm and 12 nm wide passbands and 1300 nm central wavelengths. The improvement in the signal to interference ratio (P_T/P_2) was better for incandescent radiation than for coupled radiation: 21–25 dB and 16–21 dB, respectively. The best results were obtained with a 12 nm filter, but in this case the wavelength of the light source and the filter's passband had to be individually measured and matched because of their manufacturing tolerances.

4.2. Periodic ON/OFF switching of the light source

This technique involves:
– periodic disconnection, *e.g.*, with an optical switch, or deactivation of the light source,
– two measurements in each cycle: one with the source on (P_{2I}) and another with the source off (P_T),
– subtraction of P_T from P_{2I} to obtain the true power of the test signal (P_2):

$$P_2 = P_{2I} - P_T \tag{9}$$

(power values in W).

The last operation is performed by software running on a data acquisition computer (Fig. 8). The improvement in the signal-to-interference ratio is limited by quantization errors dependent on the resolution of the power meter used, normally 0.01 dB or 0.001 dB, and the combined noise of the light source and the power meter for the time interval between the measurements of P_T and P_{2I}. Because the properties of the cable under test during fire tests tend to change slowly, as can be seen in Figs. 9–11, the duration of the ON/OFF cycle is usually measured in seconds. This allows us to perform measurements with a standard optical power meter indicating *Continuous Wave* (CW) power.

For a combined resolution and noise of 0.002 dB, equal to the minimum detectable power difference, interference from thermal radiation can be reduced by 33.36 dB with respect to its original value, but with a high level of noise in the corrected signal, approximately –3 dB. The improvement corresponding to the uncertainty of 0.05–0.20 dB in the same conditions is 20–25 dB.

4.3. Amplitude modulation (AM) of the light source

This method is in principle similar to the method presented in Section 4.2, but implemented differently:
– the modulation frequency is higher, typically 270, 1000, or 2000 Hz (fixed). Portable light sources with such ON/OFF keying are commercially available,
– an optical receiver or power meter is used capable of separating and bandpass-filtering the AC component of input power and then measuring its equivalent power. This functionality is available in some versatile benchtop power meters [24]. However, some portable power meters only indicate the presence of light modulation for the identification of fiber or test wavelength.

With no such instrument available, one can assemble a setup which usually includes a photodetector, AC amplifier, narrowband filter, and some instrument to measure amplitude of the AC signal: a digital oscilloscope, lock-in amplifier, audio level meter, *etc.* At the source side, a direct modulation of radiation from a LED or a laser is usually employed; chirp and chromatic dispersion effects can be ignored because of the low modulation frequency and a short optical path.

This method ensures high rejection of un-modulated interference encountered during fire tests. With proper choice of the modulation frequency, the low frequency noise of the photodetector and the amplifier, and the mains interference (50 or 60 Hz and harmonics) can be also eliminated.

Polarization modulation at the source is not a good choice: the state of polarization of light propagated in a single mode fiber is affected by mechanical influences on this fiber, like twisting or bending, encountered when cable burns, sags, and otherwise moves during a fire test. Additionally, the majority of fire resistant cables are multimode fibers, which support large number of modes and corresponding polarization states.

5. Conclusions

Data gathered during high temperature experiments with telecom fused silica fibers and fire tests of fiber optic cables indicate that optical fiber, especially a multimode one, heated to temperatures above approximately 900 °C becomes a source of thermal radiation of non-negligible power. The resulting interference cannot be ignored in some situations, in particular during measurements of small attenuation changes when totally misleading results are possible.

There are several relatively effective ways to eliminate or at least considerably reduce this interference. Unfortunately, current standards for testing fiber optic cables do not include a warning of this problem and recommendations on how to reduce measurement errors caused by thermal radiation in fiber under test.

References

[1] European Committee for Electrotechnical Standardization (CENELEC) (2015). *Method of test for resistance to fire of unprotected small cables for use in emergency circuits* (EN 50200). https://www.en-standard.eu/une-en-50200-2016-method-of-test-for-resistance-to-fire-of-unprotected-small-cables-for-use-in-emergency-circuits/

[2] Deutsches Institut fűr Normung (1998). Fire behaviour of building materials and elements – Part 12: Fire resistance of electric cable systems required to maintain circuit integrity – Requirements and testing (DIN 4102-12). https://www.din.de/de/mitwirken/normenausschuesse/nabau/veroeffentlichungen/wdc-beuth:din21:5407466

[3] International Organization for Standardization (2025). *Fire-resistance tests – Elements of building construction – Part 1: General requirements* (ISO 834-1:2025). https://www.iso.org/standard/83943.html

[4] European Committee for Electrotechnical Standardization (CENELEC) (2016). *Procedure to assess the circuit integrity of optical fibres in a cable under resistance to fire testing* (EN 50582:2016). https://www.en-standard.eu/bs-en-50582-2016-procedure-to-assess-the-circuit-integrity-of-optical-fibres-in-a-cable-under-resistance-to-fire-testing/

[5] International Electrotechnical Commission (2021). *Optical fibre cables – Part 1-2: Generic specification – Basic optical cable test procedures – General guidance* (IEC 60794-1-2:2021). https://webstore.iec.ch/en/publication/68394

[6] International Electrotechnical Commission (2025). *Optical fibres – Part 2-50: Product specifications – Sectional specification for class B single-mode fibres* (IEC 60793-2-50:2025). https://webstore.iec.ch/en/publication/77555

[7] International Electrotechnical Commission (2019). *Optical fibres – Part 2-10: Product specifications – Sectional specification for category A1 multimode fibres* (IEC 60793-2-10:2019). https://webstore.iec.ch/en/publication/62020

[8] Rose, A., & Bruno, T. (1998). The observation of OH in annealed optical fiber. *Journal of Non-Crystalline Solids*, *231*(3), 280–285. https://doi.org/10.1016/s0022-3093(98)00676-0

[9] Yu, L., Homa, D., Ohodnicki, P., Buric, M., Chorpening, B., Pickrell, G., & Wang, A. (2019). Thermally induced emission from hydroxyl groups in fused silica optical fibers. *Optical Fiber Technology*, *52*, 101951. https://doi.org/10.1016/j.yofte.2019.101951

[10] Borzycki, K., Jaworski, M., & Kossek, T. (2021). High temperature effects in fused silica optical fibers. *Journal of Telecommunications and Information Technology*, *3*(2021), 56–71. https://doi.org/10.26636/jtit.2021.153521

[11] Humbach, O., Fabian, H., Grzesik, U., Haken, U., & Heitmann, W. (1996). Analysis of OH absorption bands in synthetic silica. *Journal of Non-Crystalline Solids*, *203*, 19–26. https://doi.org/10.1016/0022-3093(96)00329-8

[12] Yu, L., Bonnell, E., Homa, D., Pickrell, G., Wang, A., Ohodnicki, P., Woodruff, S., Chorpening, B., & Buric, M. (2016). Observation of temperature dependence of the IR hydroxyl absorption bands in silica optical fiber. *Optical Fiber Technology*, *30*, 1–7. https://doi.org/10.1016/j.yofte.2016.01.004

[13] Shikama, T., Toh, K., Nagata, S., Tsuchiya, B., & Ohno, Y. (2008). Temperature measurement by thermal luminescence of partially replaced core optical fiber. *Journal of Nuclear Materials*, *386–388*, 1023–1026. https://doi.org/10.1016/j.jnucmat.2008.12.204

[14] International Telecommunication Union (2024). *Characteristics of a single-mode optical fibre and cable*. (ITU-T G.652:2024-08). https://www.itu.int/rec/T-REC-G.652-202408-I

[15] Rose, A. (1997). Devitrification in annealed optical fiber. *Journal of Lightwave Technology*, *15*(5), 808–814. https://doi.org/10.1109/50.580819

[16] Homa, D., Pickrell, G., & Wang, A. (2018). Investigation of High Temperature Silica Based Fiber Optic Materials (Final Report). https://doi.org/10.2172/1489125

[17] Borzycki, K., Jaworski, M., & Kossek, T. (2023). Remedies to thermal radiation in fused silica optical fibers. *Journal of Telecommunications and Information Technology*, *1*(2023), 88–96. https://doi.org/10.26636/jtit.2023.166222

[18] Honda, A., Toh, K., Nagata, S., Tsuchiya, B., & Shikama, T. (2007). Effect of temperature and irradiation on fused silica optical fiber for temperature measurement. *Journal of Nuclear Materials*, *367–370*, 1117–1121. https://doi.org/10.1016/j.jnucmat.2007.03.193

[19] European Committee for Electrotechnical Standardization (CENELEC) (2014). Power, control and communication cables. Cables for general applications in construction works subject to reaction to fire requirements (EN 50575:2014). https://standards.iteh.ai/catalog/standards/clc/b8675c9d-b3b4-4a46-ae9e-7207aca441cb/en-50575-2014

[20] International Electrotechnical Commission (2024). *Optical fibres – Part 1-40: Attenuation measurement methods* (IEC 60793-1-40:2024). https://webstore.iec.ch/en/publication/103854

[21] International Electrotechnical Commission (2024). *Optical fibres – Part 1-46: Measurement methods and test procedures – Monitoring of changes in optical transmittance* (IEC 60793-1-46:2024). https://webstore.iec.ch/en/publication/96235

[22] Telecommunications Industry Association (2016). Detail Specification for 50 µm Core Diameter/125 µm Cladding Diameter Class 1a Graded Index Multimode Optical Fibers with Laser-Optimized Bandwidth Characteristics Specified for Wavelength Division Multiplexing (TIA-492AAAE:2016). https://store.accuristech.com/standards/tia-tia-492aaae?product_id=2592718

[23] International Electrotechnical Commission (2017). *Optical fibre cables – Part 1-2: Generic specification – Basic optical cable test procedures – General guidance* (IEC 60794-1-2:2017). https://webstore.iec.ch/en/publication/33149

[24] Model 1936-R/2936-R Series. Single and Dual-Channel Optical Meters. User's Manual. Newport Corporation, Part No. 90039770 rev B, 2008.

Krzysztof Borzycki received his Ph.D. degree in telecommunication engineering from the National Institute of *Telecommunications* (NIT), Warsaw, Poland, in 2006. He is currently an assistant professor with the NIT Telecom Measurements Department. His research, consulting, standardization, and training activities cover optical fibers, cables and passive components, fiber access networks, as well as testing and characterization of these. He has authored or co-authored 48 papers in journals, 28 conference papers, and 7 book chapters. He is a NIT representative of the "Cables and Wires" and "Fiber Optics" Technical Committees in the Polish National Standards Committee.